Novel method to study SOL-response to ELMs by divertor target probes in JET

S. Jachmich[1], M. Laux[2], M. Becoulet[3], T. Eich[4], A. Loarte[3], G. Matthews[3], V. Phillips[4], W. Fundamenski[3], M. Stamp[3] and contributors to the EFDA-JET workprogramme

[1] *Laboratory for Plasma Physics, Ecole Royale Militaire/Koninklijke Militaire School, Association "Euratom-Belgian State", Brussels, Belgium*[*]

[2] *Max-Planck-Institut für Plasmaphysik, Association EURATOM, Bereich Plasmadiagnostik, Berlin, Germany*

[3] *UKAEA Fusion, Culham Science Center, Abingdon,UK*

[4] *Institut für Plasmaphysik, Forschungszentrum Jülich, Jülich, Germany*[*]

[*] Partners in the Trilateral Euregio Cluster (TEC)

1. Introduction

The particle fluxes and heat energy loads, which accompany edge localised mode phenomena (ELM) during high confinement discharges cause losses in density and plasma energy and may lead to enhanced erosion of the divertor target plates. In the past the global properties and scalings of the ELMs have been explored [1,2]. However, the underlying physics is still concealed due to the stochastic nature, of which ELMs are. In order to reveal detailed time information of a *typical ELM*, a new ELM identification algorithm has been applied to ELMy H-mode periods to find ELM parameters in the D_α signal and in I_{sat}, V_{float} and T_e from triple probes in the divertor targets. Once an ELM-event has been identified, the inverse time interval of successive ELM events, the width, height and integral of the ELM burst, and the average signal between ELMs is calculated for every individual ELM in the series. In addition, the data of all ELMs, which belong to the same phase during an ELM, are combined and averaged. The so reconstructed time trace, which represents a typical ELM, is discussed in more detail elsewhere [3]. In order to discover and to exclude irregular ELMs, their total deviation to the averaged ELM is determined. For the calculation of more complex plasma quantities, which consist of different diagnostics, one signal is used as a marker and a second one is averaged accordingly to the first one. In most cases the D_α recycling has been used as a marker signal, since it shows usually a very sharp peak.

2. Changes of individual ELM parameters during H-mode discharge

From an H-mode discharge (I_p= 3 MA, P_{tot} = 15 MW, $\langle n_e \rangle_0$=2.8 10^{19} m^{-3}) the series of ELMs, which is indicated in Figure 1, has been extracted and analysed. It is obvious that the ELM-frequency is slightly increasing in time. A simple relation between the time since the last ELM and the peak area of the subsequent ELM seems to hold at least in a statistical sense. The postulate that more particles accumulate until the next ELM-event is triggered leads to an inverse proportionality between the peak area and the ELM-frequency. This is

confirmed in Figure 2, where the D_α peaks are decreasing with the inverse time between ELMs. The ratio of the peak to the background flux decreases until an almost constant level is achieved.

The individual standard deviation of all ELMs with respect to the averaged one is very small (2-6%!, see Fig. 3). This proves that the averaged ELM is in fact the *typical ELM* of this series (shown in Fig. 4, where also the individual ELMs are plotted). However it becomes also clear that there are four exceptional ELMs present. Those short and small additional peaks in D_α are strewn in between the regular ELMs on a surprisingly regular time pattern with a period of 77 ms, which is much lower than the present ELM-frequency. The deviation of the ion saturation current from the average ELM is reasonably small (5-10%), but for the floating potential and electron temperature it is higher (respectively 10-40%, 30-200%).

In some cases the post-ELM signals do not return to their pre-ELM values until the next ELM approaches and, therefore, higher particle flux and electron temperature can build up. This non-stationary behaviour usually leads to a transition in ELM type. Both probes on the outer target exhibit such features (Fig. 5). The gradient of the SOL-profile is at the ELM-burst higher than in between ELMs.

3. Detailed temporal evolution of an ELM

The electron temperature and floating potential are peaking during the rise of the particle flux (Fig. 6). This early rise leads to broadening or even to a multiple peak structure of the power load Q_p (Fig. 7), which has been derived by assuming a sheath transmission factor γ of 8 (with $T_i=T_e$). Although the electron temperature reaches in maximum 30-40 eV, the applied voltage is sufficient to measure the I_{sat}-current. The so measured power flux represents the heat flow due to the electrons. Despite a possible change of γ due to higher T_i or T_e, the rate of change is small enough to assure a good measurement of Q_p. Since no probe was located at the separatrix, it is not possible to derive the spatially maximum power load. Comparisons with IR-data are underway. More information can be found in [4].

If strong gas puffing is applied the peaks are broadened. Although the gas has been released into the inner divertor base, also the outer divertor recycling seems to be influenced by the neutrals (Fig. 8). At low power crossing the separatrix or at low densities the double peak seen in the power flux can also be present in D_α as it is illustrated in Figure 9. Comparisons with the ion saturation current confirmed this observation.

4. Conclusions

ELMs can be studied in a more systematic manner by averaging probe signals using a common marker signal for an event. The relatively small standard deviations of the single ELMs from the averaged one demonstrated clearly the fact that the ELMs appear in a very regular manner, which makes such analysis feasible. The technique can be applied to any measured quantity and thus allows the calculation of even more complex plasma quantities. A first analysis has shown an early rise in T_e and V_{fl}, which is in contradiction to the delayed I_{sat}-rise and therefore indicates a double peak structure of the power load. The heat flux

consists of two components: an early short small pulse of hot particles, followed by a longer large one at much lower temperature.

The study of inner/outer divertor recycling asymmetries has elucidated particle fluxes, which appear after the ELM burst at lower time scales. Depending on the density and gas puffing, they are seen either on the outer or on the inner divertor box.

The results presented here are only a small collection of the detailed ELM-behaviour. In order to retrieve more information it is planned to extend the procedure to slow probe voltage ramps and slow X-point sweeps. In the first case I(V)-characteristics can be reconstructed for each ELM time, in the second changes of the SOL-profiles during an ELM can be analysed.

References

[1] JET Team, Nucl. Fusion **39** (1999), 1687.

[2] G. Saibene *et al.*, Nucl. Fusion **39** (1999), 1133.

[3] M. Laux *et al.*, this conference.

[4] Th. Eich *et al.*, this conference.

Figures

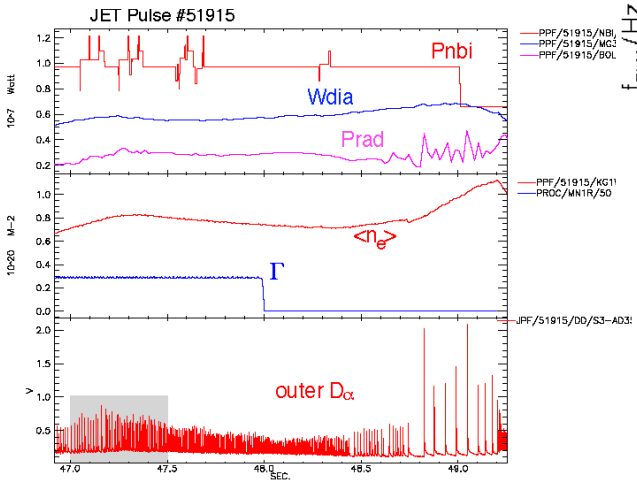

Fig. 1: Time traces of neutral beam power, plasma diamagnetic energy, radiated power, line integrated central density, gas flow Γ and recycling at the outer divertor box (D_α). The grey shaded box indicates the series of analysed ELM.

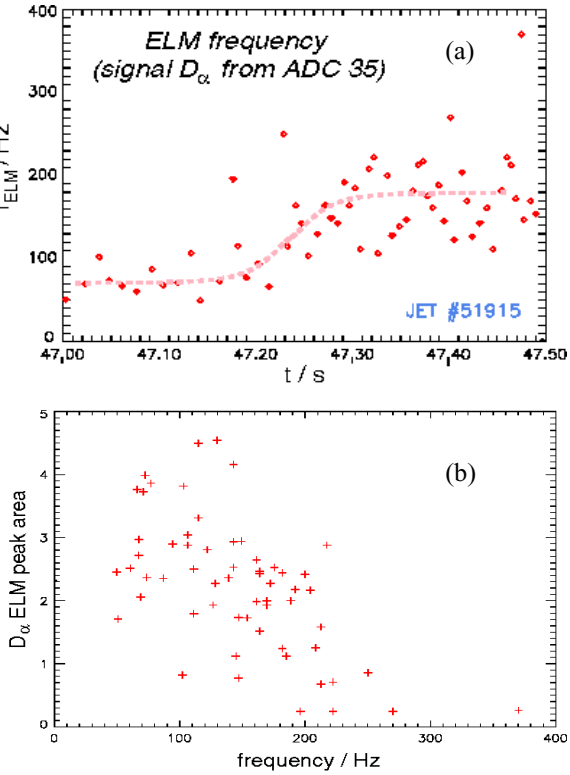

Fig. 2: (a) changes of the ELM-frequency. (b) area of ELM peak decreases with frequency.

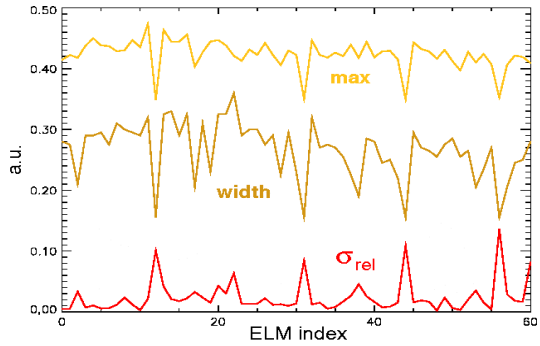

Fig. 3: Peak maximum, peak width and standard deviation of each ELMs. The four spikes in σ_{rel} occur on a regular time pattern.

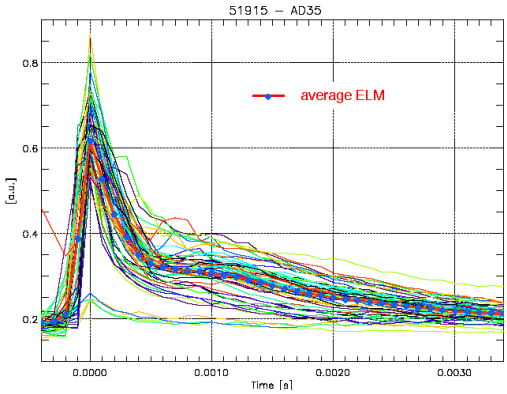

Fig. 4: All individual ELMs and the resulting average ELM. Note the four small exceptional ELM-events.

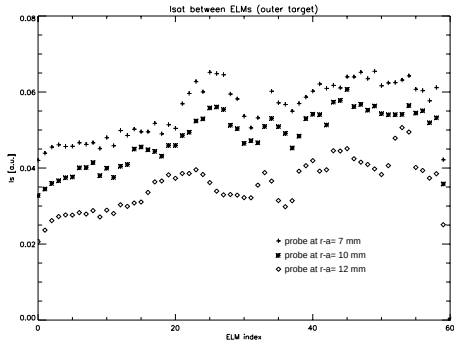

Fig. 5: Ion saturation current in between ELMs of three probes at the outer target is increasing in time.

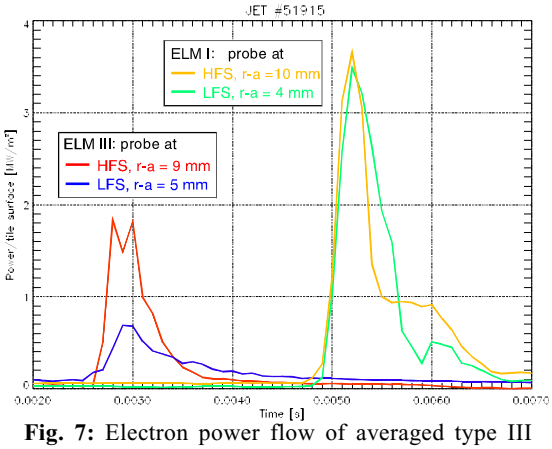

Fig. 7: Electron power flow of averaged type III ELMs (t=47-47.5) and during type I ELMs (t=48.8-49.2). The type I are plotted with an arbitrary time offset.

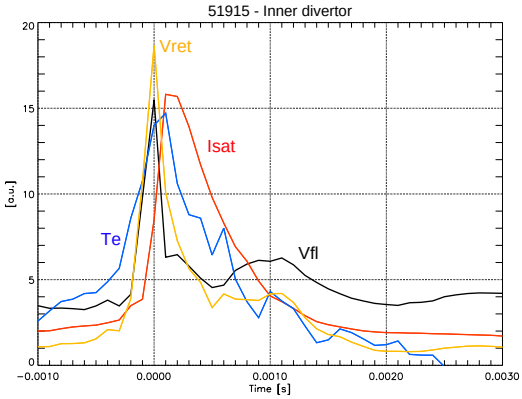

Fig. 6: Ion saturation current, floating potential, return voltage and electron temperature of average ELM. The peak of I_{sat} is delayed.

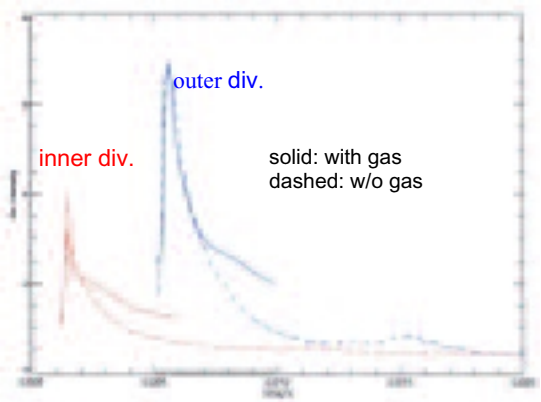

Fig. 8: Average ELM course of D_α with and w/o gas-puff. The humps in the solid curves indicate a second particle flow during strong gas puffing.

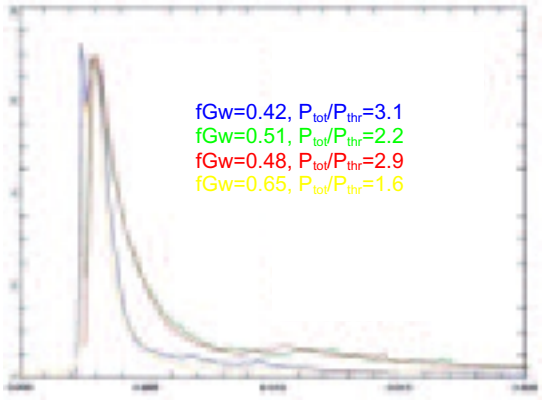

Fig. 9: Average ELM course of D_α for various density and separatrix power. Note the pre-peak for low n_e or/and low P_{sep}.